Hindawi Publishing Corporation
EURASIP Journal on Wireless Communications and Networking
Volume 2007, Article ID 19196, 16 pages
doi:10.1155/2007/19196

Research Article

Impact of Radio Link Unreliability on the Connectivity of Wireless Sensor Networks

Jean-Marie Gorce, Ruifeng Zhang, and Hervé Parvery

ARES INRIA / CITI, INSA-Lyon, 69621 Villeurbanne Cedex, France

Received 30 October 2006; Revised 30 March 2007; Accepted 6 April 2007

Recommended by Mischa Dohler

Many works have been devoted to connectivity of *ad hoc* networks. This is an important feature for wireless sensor networks (WSNs) to provide the nodes with the capability of communicating with one or several sinks. In most of these works, radio links are assumed ideal, that is, with no transmission errors. To fulfil this assumption, the reception threshold should be high enough to guarantee that radio links have a low transmission error probability. As a consequence, all unreliable links are dismissed. This approach is suboptimal concerning energy consumption because unreliable links should permit to reduce either the transmission power or the number of active nodes. The aim of this paper is to quantify the contribution of unreliable long hops to an increase of the connectivity of WSNs. In our model, each node is assumed to be connected to each other node in a probabilistic manner. Such a network is modeled as a complete random graph, that is, all edges exist. The instantaneous node degree is then defined as the number of simultaneous valid single-hop receptions of the same message, and finally the mean node degree is computed analytically in both AWGN and block-fading channels. We show the impact on connectivity of two MACs and routing parameters. The first one is the energy detection level such as the one used in carrier sense mechanisms. The second one is the reliability threshold used by the routing layer to select stable links only. Both analytic and simulation results show that using opportunistic protocols is challenging.

1. INTRODUCTION

Wireless sensor networks (WSNs) have generated a tremendous number of original publications over the last decade. When compared to other *ad hoc* networks, WSNs differ by their constraints. The leading constraint unquestionably is the life time of the network which is closely related to energy consumption. One approach for increasing life time consists of providing the nodes with sleeping periods [1–3], under the constraint that sensing function and connectivity are preserved [4]. Optimizing routing protocols is an important task which requires connectivity of the network [5]. Many works have studied the connectivity of *ad hoc* networks [6–9]. Pioneering works dealing with network connectivity [10, 11] are based on a perfect geometric disk model; that is, all links are reliable and occur only when the communication distance is lower than a threshold, the radio range. Other more recent works are founded on this assumption, providing numerous wireless network connectivity bounds. In [7, 9, 12], the connectivity is assessed for a large random network providing asymptotic rules. Hence, in [9] an asymptotic minimal range $R(n)$ for granting connectivity is derived for the case of n nodes randomly distributed in a disc of unit area. The minimal range is obtained as $R(n)^2 \geq (\log n + c(n))/\pi \cdot n$ with $c(n) \to \infty$ when $n \to \infty$. A pure geometric approach is used in [13] to provide an exact analytical derivation for a 1D ad hoc network. This result further grants a bound for 2D radio networks.

Important to our work is the contribution of [14] studying the mean node degree of WSNs and the isolation node probability. In [15] the authors show how the isolation node probability well approximates the connectivity probability.

Most of these already published works are based on the perfect geometric disc model as illustrated in Figure 1(a). This model relies on the following three fundamental axioms.

(i) Switched link: the radio link is assumed boolean: two nodes are either perfectly connected, or out of range.
(ii) Circular geometric neighborhood: the received power solely depends on the transmitter-receiver distance.
(iii) Interference free: each radio link is assumed independent from each other.

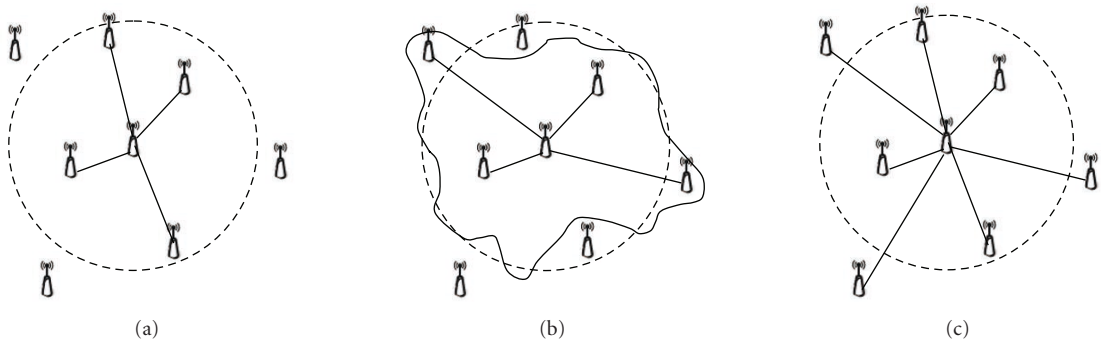

Figure 1: Node's neighborhood with different radio link models: (a) perfect unit disk, (b) switched links with shadowing, (c) unreliable links accounting for transmission errors. With this latter model, all nodes are neighbors with a given successful transmission probability, visualized by the lines' thickness.

Recent works advocate the need of more realistic radio link models (see, e.g., [12, 16–20]).

Concerning connectivity, the second axiom (i.e., *circular coverage*) has been relaxed in recent studies [21–23] and the impact of log shadowing is evaluated. The coverage areas are deformed as illustrated in Figure 1. Under this model, each coverage area is squeezed and stretched (see Figure 1(b)) independently, but the neighborhood is still on average a circular function. This is because the deformation is introduced as an uncorrelated process. The most important result issued from these works is that path-loss variations help to maintain the network connectivity. The radiation pattern is another factor which can affect the second axiom [24]. As detailed in [25], radiation pattern can also improve both connectivity and capacity.

The third axiom (*interference free*) has been relaxed in a recent work. Reference [26] rests on the approximation that interference acts as additive Gaussian noise. It follows that a transmission succeeds only if the signal to interference plus noise ratio (SINR) exceeds the reception threshold.

All these works assume that the first axiom is true, thus needing the definition of a reception threshold. This hypothesis is justified by information theory. Basically, the successful transmission probability, having a radio link distance d, namely $P_s(\mathrm{tr}|d)$, is a decreasing function which stiffens and gets closer to a step function provided that ideal (but long) channel coding is used. However, an infinite length code would be necessary to reach exactly the switched link model. With a rather realistic short-length channel coding, there is always a region in which nodes have a reception probability neither null nor certain, as illustrated in Figure 2 [27, 28].

Noisy links were introduced in [29] in the framework of graph theory and percolation. They show that the overall connectivity improves when new links beyond the range just make up for broken links above.

This paper aims at studying the unreliability of radio links in the intermediate region to quantify their leading role in the connectivity. In our model, any node has a probability to receive any message as illustrated in Figure 1(c). This probability tends towards 1 for near communication and towards 0 when distance goes to infinity. With such a realistic model, the communication range becomes undefined and is replaced by a reception probability law depending on the distance. This law relies on various parameters such as channel propagation model, radio transmission technique (packets-size, modulation, coding, etc.), and packet size.

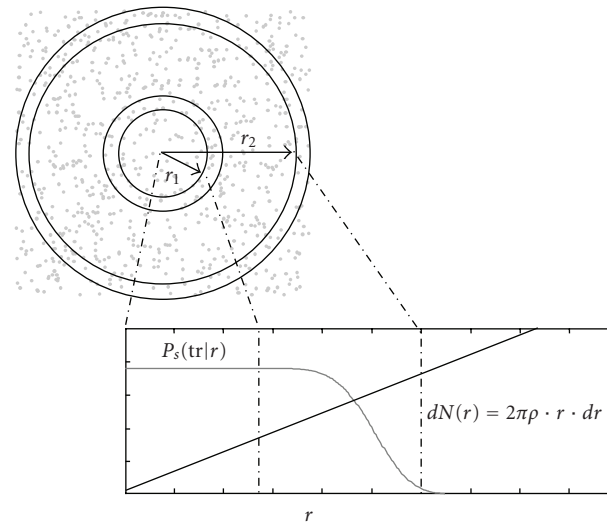

Figure 2: The neighbors are considered placed in rings centered at the transmitter. The mean number of successful hops of length r results from the product of the success probability (gray line) having $\gamma(r)$, and the number of nodes (black line) in a differential ring of thickness dr and radius r.

Section 2 provides a short overview of previously published works [14, 15, 21–23] dealing with connectivity having switched radio links. The mean node degree definition is extended to unreliable radio links in Section 3 and an overall expression for the probabilistic radio link is provided. Also, the mean node degree is described from a cross-layer point of view in Section 3.3 by introducing two parameters from MAC and routing layers. The first one is the energy detection level such as the one used in a carrier sense mechanism.

The second one is the reliability threshold which can be used at the routing layer to select stable links only. The theory derived in this section is then deeply studied in Section 4, firstly for additive white gaussian noise (AWGN) channels and then broadened to block-fading channels modeled by Nakagami-m distributions. A closed-form lower bound of the mean node degree is found and expressed as a function of the energy detection level and the reliability threshold. The accuracy of our results is evaluated using extensive simulations in Section 5. Some conclusions and perspectives are drawn in Section 6.

2. CONNECTIVITY: A STATE OF THE ART

2.1. Connectivity versus mean node degree

This section provides the reader with some previously published definitions and connectivity properties of switched-link-based WSNs for the sake of consistency. A switched link model is based on the assumption that the transmission between two nodes x and x' succeeds if and only if the signal-to-noise ratio (SNR) $\overline{\gamma}(x,x')$ at the receiver is above a minimal value $\overline{\gamma}_{\min}$. The widely used disk range model is then achieved if one assumes the antennas are all omnidirectional and the radio wave propagates isotropically. For the sake of simplicity, all the devices are assumed to be transmitting at the same power level P_t.

The nodes of the WSN are further assumed independent and randomly distributed according to a random point process of density ρ, over the space R^2. The WSN is further considered spread over an infinite plan, to avoid boundary problems. The probability of finding N nodes in a region A follows a two dimensional Poisson distribution:

$$P(n \text{ nodes in } S) = P(N = n) = \frac{(\rho \cdot S_A)^n}{n!} e^{-\rho \cdot S_A}, \quad (1)$$

with $E[N] = \rho \cdot S_A$.

This process is usually studied using its associated random graph $G_{p(x,x')}(N)$ model, where N is the number of nodes, and $p(x,x')$ the probability of having a link (edge) between two nodes positioned at x and x', respectively. A pure random graph has $p(x,x') = p_0$ while a random geometric graph has $p(x,x') = 1$ for $|x - x'| < R$. The later represents an ideal radio network well, with range R—see Figure 1(a).

A WSN roll out is defined as a particular realization of the random process and is represented by a deterministic graph $G = \{V, L\}$, where V and L are, respectively, the set of nodes and the set of valid radio links $l(x,x')$. Under the hypothesis of switched links, $l(x,x')$ only exists if both are in range one of each other.[1]

The connectivity is an important feature for WSNs. A graph is said to be connected if at least one multihop path exists between all pairs of nodes in the graph. Note that the sensors can all communicate with a unique sink if and only if the corresponding graph is connected.

This connectivity cannot be formally expressed as the probability of having $G = \{V, L\}$ connected because the random process herein used is spread over an infinite plan. The number of nodes thus tends toward infinity. In [29], the connectivity is defined as the probability of having an infinite connected component in G. In [8, 9], the network is scaled down to a finite disk area, and the connectivity is assessed thanks to the range $R(n)$ which allows to make the graph asymptotically connected (i.e., for $n \to \infty$). In [21], the connectivity is also studied in a finite disk but defined as a subregion of a whole infinite network at a constant density. This definition is substantially different, because the nodes outside the disk can help for the connectivity of nodes inside the disk. Then, connectivity is assessed through the probability $P(\text{con}(A))$ that the nodes inside a subarea A of surface S_A are connected one to each other.

In this paper, we adopted this latter definition. This probability cannot be analytically derived from the properties of the random process and an upper bound is instead found by stating that the nodes in region A are obviously not connected if at least one node is isolated:

$$P(\text{con}(A)) \le P(\overline{\text{ISO}}(A)), \quad (2)$$

where $\text{con}(A)$ is true if all nodes in A are connected, and $\overline{\text{ISO}}(A)$ is true if no one is isolated.

$P(\overline{\text{ISO}}(A))$ is thus the probability of having no node isolated in A. This upper bound is known to be tight for either random geometric or pure random graphs, at least for high connectivity probability. The tightness of the bound is not proven in a broadened framework.

$P(\overline{\text{ISO}}(A))$ is derived in [21, 23] assuming the isolation of nodes to be almost independent events, providing

$$\begin{aligned} P(\overline{\text{ISO}}(A)) &= \sum_{n=0}^{\infty} P(\text{ISO}(A) | N = n) \cdot P(N = n) \\ &= \exp\big(-\rho \cdot S_A \cdot P(\text{iso})\big), \end{aligned} \quad (3)$$

where $P(\text{iso})$ is the node isolation probability.

Let the node degree $\mu(x)$ be defined as the number of links of a node x, the mean value being referred to as μ_0. $P(\text{iso})$ is simply equal to the probability of having $\mu(x) = 0$, and thus

$$P(\text{iso}) = \exp\big(-\mu_0\big). \quad (4)$$

The close relationship between connectivity and mean node degree can now be stated by introducing (4) and (3) in (2):

$$P(\text{con}(A)) \le \exp\big(-\rho \cdot S_A \cdot e^{-\mu_0}\big). \quad (5)$$

Starting from this bound, the remainder of this paper focuses on the mean node degree property. The tightness of (5) is investigated by simulation in Section 5.3.

[1] It should be noted that in this work and other referenced works in this paper, radio links are assumed symmetrical, and thus associated graphs are undirected.

2.2. Mean node degree with the perfect disc model

The degree expectation of a node x relies on the radio links according to

$$\overline{\mu}(x) = \int_{x' \in R^2} l(x, x') \cdot f_x(x') dx', \tag{6}$$

where $f_x(x')$ is the probability density function of having a node in x'. This is because the nodes are uniformly distributed, $f_x(x') = \rho$ and the process is ergodic. Spatial and time expectations then converge to the same value given by

$$\mu_0 = \overline{\mu}(x) = \rho \cdot \int_{x' \in R^2} l(x, x') dx'. \tag{7}$$

The exact expression of $l(x, x')$ relies on the propagation model. Usefulness for our ongoing development is to derive the link as a function of the SNR defined by

$$\overline{\gamma}(x, x') = \frac{E_b(x, x')}{N_0}, \tag{8}$$

with N_0 the noise power density of the receiver which is assumed constant for all nodes. $E_b(x, x')$ is the received energy per bit given by $E_b(x, x') = T_b \cdot P_r(x, x')$ where T_b is the bit period. $P_r(x, x')$ is the received power given by

$$P_r(x, x') = \frac{P_t(x)}{L(x, x')}, \tag{9}$$

where $L(x, x')$ is the path loss between x and x'.

The usual disc range model is achieved when $L(x, x')$ is considered a homogeneous and isotropic function $L(x, x') = L(d_{xx'})$, where $d_{xx'}$ is the geometric distance between x and x'. The single slope path-loss model is defined by

$$L(d_{xx'}) = L(d_0) \left(\frac{d_{xx'}}{d_0} \right)^{\alpha} \tag{10}$$

having the path loss exponent α usually ranging from 2 (free space) to 6. $L(d_0)$ is the arbitrary path-loss reference at distance d_0.

Plugging this model into (7) yields

$$\mu_0 = 2\pi \cdot \rho \cdot \int_{s=0}^{\infty} l(d_{xx'} = s) \cdot s \cdot ds \tag{11}$$

with

$$l(d_{xx'}) = \mathbf{1}(\overline{\gamma}(x, x') \geq \overline{\gamma}_{\min}) = \mathbf{1}(d_{xx'} \leq d_{\max}), \tag{12}$$

where $\mathbf{1}(x)$ is a logical function, equal to 1 if x is true. One has $d_{\max} = d_0 \cdot (\overline{\gamma}_0 / \overline{\gamma}_{\min})^{1/\alpha}$ and $\gamma_0 = T_b \cdot P_t(x)/N_0 \cdot L(d_0)$.

Such a model leads to the well-known perfect disc range model (see Figure 1(a)) where (11) reduces to

$$\mu_0 = \pi \cdot \rho \cdot d_{\max}^2. \tag{13}$$

2.3. Mean node degree with shadowing

The physical layer model can be enhanced using a more realistic propagation model [21, 23], taking into account spatial path loss variations due to obstacles [30], as illustrated in Figure 1(b). A usual way consists of introducing a second term to the deterministic path loss: the statistical shadowing component usually considers "log normally" distributed around its mean value [31] according to

$$L^{(\mathrm{dB})}(x, x') = L_{50\%}^{(\mathrm{dB})}(d_{xx'}) + L_{\mathrm{sh}}^{(\mathrm{dB})}(d_{xx'}), \tag{14}$$

where $L_{50\%}^{(\mathrm{dB})}(d_{xx'}) = 10 \cdot \log_{10}(L(d_{xx'}))$, from (10), is the median path-loss value. $L_{\mathrm{sh}}^{(\mathrm{dB})}(d_{xx'})$ refers to a zero mean Gaussian random variable with standard deviation σ_{sh}, proportional to the shadowing strength. Its probability density function (pdf) is given by

$$f\left(L^{(\mathrm{dB})}(x, x')\right) = \frac{1}{\sqrt{2\pi}\sigma_s} \exp \frac{-\left(L^{(\mathrm{dB})} - L_{50\%}^{(\mathrm{dB})}(d_{xx'})\right)^2}{\sigma_s^2}. \tag{15}$$

Combining (8) and (10) into (15) provides the pdf $f_{\gamma}(\gamma|\cdot)$ as

$$f_{\overline{\gamma}}(\overline{\gamma}|d_{xx'}) = \frac{10}{\ln 10} \gamma^{-1} \cdot f\left(L(d_{xx'})\right). \tag{16}$$

The shadowing distorts the perfect disc neighborhood. However, once one has the shadowing effect computed, each radio link $l(x, x')$ stays constant: the corresponding graph is thus deterministic. While the random process is still isotropic, each realization is not.

The mean node degree in (7) is now replaced by

$$\mu_0 = 2\pi \cdot \rho \cdot \int_{s=0}^{\infty} P\left(l(d_{xx'} = s)\right) \cdot s \cdot ds, \tag{17}$$

with

$$P\left(l(d_{xx'})\right) = P\left(\overline{\gamma}(d_{xx'}) > \gamma_{\min}\right) = \int_{\overline{\gamma} = \gamma_{\min}}^{\infty} f_{\overline{\gamma}}(\overline{\gamma}|d_{xx'}) d\overline{\gamma}. \tag{18}$$

This problematic has been studied in both [21, 23].

This overview stresses out the leading role of the mean node degree in the connectivity of WSNs. Some more recent works have also proposed to broaden this result by introducing fading and even radiation patterns. Basically these works rest on the adaptation of $l(x, x')$ to a spatially variable function. The neighborhood is *stretched and squeezed* [29] but still based on a switched radio link assumption.

3. CONNECTIVITY UNDER UNRELIABLE RADIO LINKS

3.1. Time-varying node degree

The use of a realistic radio link modifies in depth the connectivity of WSNs described above. A realistic radio link refers to a radio link having a certain error probability. Because the radiated power density decreases with distance, there is always

a given range for which the nodes are neither good neighbors, nor unknown. This has a large impact on both mean node degree and connectivity.

We consider as in [29] a random connection model where each radio link $l(x, x')$ is probabilistic. The radio link is thus defined as successful transmission probability between two nodes:

$$l(x, x') = P_s(\mathrm{tr}|x, x'); \quad P_s(\mathrm{tr}|x, x') \in [0, 1]. \tag{19}$$

In the previous model, nodes were randomly distributed but each radio link in a particular realization was considered deterministic. Now, the following definition holds.

Definition 1. A WSN is defined as a realization of a Poisson point random process. Each node is a possible neighbor of each other with a given probability. The random graph $G_p(N, L)$ associated with each particular realization is thus complete (all edges exist). Each edge, $l(x, x') \in L$, relates to the successful transmission probability.

The main difference with the previous model is that a realization of the process (a set of randomly rolled-out nodes) is now itself a random graph as illustrated in Figure 1(c). Each time a node sends a packet to the sink, a new graph is experienced by the WSN. This graph is now referred to as $G(N, L_\tau)$, where L_τ is the set of successful transmissions in the WSN at time τ denoted $l_\tau(x, x')$.

With this model, the probability of having a successful long hop may not be negligible despite the fact that the transmission probability decreases with distance d. This decreasing probability can be indeed compensated for by the increasing number of nodes in a ring of constant thickness δ and of radius d (see Figure 2). The connectivity is still evaluated as the probability that a given subset of nodes is connected. The following definition is first stated.

Definition 2. The instantaneous node degree $\mu(x, \tau)$ is defined as the number of simultaneous successful transmissions experienced at time τ by a transmitter located in x:

$$\mu(x, \tau) = \sum_{x'} l_\tau(x, x') \tag{20}$$

and then the following definition holds.

Definition 3. The mean node degree $\overline{\mu}(x)$ is the expected value of $\mu(x, \tau)$ with respect to time

$$\overline{\mu}(x) = E_\tau(\mu(x, \tau)) = \sum_{x'} l(x, x'), \tag{21}$$

where one has $l(x, x') = E_\tau(l_\tau(x, x'))$.

Because the process is ergodic (statistical properties are stationary in time and space), the expectation with respect to space converges to the same value and is given by

$$\mu_0 = E_{x,\tau}(\mu(x, \tau)) = \rho \cdot \int_{x' \in R^2} l(x, x')dx'. \tag{22}$$

Equation (22) is similar to (7) but with having $l(x, x')$ probabilistic.

3.2. A realistic radio link

The radio link is defined equal to the transmission probability $l(x, x') = P_S(\mathrm{tr}|\gamma(x, x'))$, having

$$P_S(\mathrm{tr}|\gamma) = (1 - \mathrm{BER}(\gamma))^{N_b}, \tag{23}$$

where N_b is the number of bits per frame and $\mathrm{BER}(\gamma)$ the bit error rate. This BER depends on modulation, coding, and more generally on transmitting and receiving techniques (diversity, equalization, etc.). It should also rely on the channel impulse response, but selective fading is not considered in this work.

Flat fading is more important because it is often present in confined environments where WSNs could be rolled out. The flat fading accounted for by multipath propagation leads to fast variations of received power due to the incoherent summation of multiple waves. From a general point of view, the transmission probability can be estimated from the mean BER given by

$$\mathrm{BER}_f(\overline{\gamma}) = \int_0^\infty \mathrm{BER}(\gamma) \cdot f_\gamma(\gamma|\overline{\gamma})d\gamma, \tag{24}$$

which can be bounded in many practical situations [32]. $f_\gamma(\gamma|\overline{\gamma})$ is the pdf of γ having a mean SNR $\overline{\gamma}$, representing the fast fluctuations of received power.

However, in slow varying channels—as occurring with fixed WSNs and short packets—the channel can be assumed constant within a packet duration. Under such an assumption, referred to as pseudo stationarity, the channel is called a block-fading channel. In this case, the successful transmission probability does not rely on (24) but directly on (23) according to

$$P_S(\mathrm{tr}|\overline{\gamma}) = \int_{\gamma=0}^\infty P_S(\mathrm{tr}|\gamma) \cdot f_\gamma(\gamma|\overline{\gamma}) \cdot d\gamma. \tag{25}$$

As done in the previous section, propagation (10) and shadowing (16) are plugged into the expectation of (25), yielding

$$P(l(d_{xx'})) = \int_{\overline{\gamma}=0}^\infty \int_{\gamma=0}^\infty P_S(\mathrm{tr}|\gamma) \cdot f_\gamma(\gamma|\overline{\gamma}) \cdot f_{\overline{\gamma}}(\overline{\gamma}|d_{xx'}) \cdot d\gamma \cdot d\overline{\gamma}. \tag{26}$$

The more general mean node degree expression is now given by (17) in which (18) is replaced by (26).

3.3. A cross-layer point of view

From a cross-layer point of view, the mean node degree can be modified to take some MAC and routing features into account.

The power detection level of an incoming signal is an important PHY parameter which the MAC layer can possibly assess. A carrier sense mechanism—or any other energy detection mechanism—is used at PHY for providing the MAC with the channel state. The key parameter is the energy detection level, or equivalently the SNR threshold denoted ε_d at which the receiver switches to active reception mode. Such a

mechanism can be easily introduced in (26) as a lower bound in the integration with respect to γ. Indeed, the radio link probability becomes null when $\gamma < \varepsilon_d$ since the incoming signal is not detected.

Neighborhood management to maintain routes over the network is seen as a routing layer issue, exploiting a link layer information. Routing algorithms, either active or proactive, often consider radio links as reliable and stable enough so that a route can be established for a reasonable duration. This stability can be questionable in real environments. The shadowing effect can be assumed stationary because the WSN is fixed, but the fading effect should be considered time-varying because it is sensitive to very small displacements of either the nodes or surrounding objects. Fading is however assumed to be constant for the duration of a packet, but totally uncorrelated between successive ones.

The reliability of a link is given by the successful transmission probability, and is extracted from (26) as follows:

$$P_s(\mathrm{tr}|\overline{\gamma}) = \int_{\gamma=\varepsilon_d}^{\infty} P_s(\mathrm{tr}|\gamma) \cdot f_\gamma(\gamma|\overline{\gamma}) \cdot d\gamma. \tag{27}$$

The link layer can thus estimate the link reliability by only knowing the mean SNR $\overline{\gamma}(x, x')$, using (27). The routing layer can then remove unreliable nodes from its neighborhood, which are those having a mean SNR below a given threshold $\overline{\gamma}_r$ defined such as $P_s(\mathrm{tr}|\overline{\gamma}_r) < P_{\mathrm{rel}}$ where P_{rel} is the target minimal success probability. This threshold should be high for proactive protocols which require stable routes but may be eventually very low for opportunistic routing protocols such as those used for geographic based routing [33]. In the latter case, all nodes receiving a packet are potentially retransmitters, and thus they can all be involved in the transmission process, even if their reception probability is very low. Thus, the full node degree can be exploited, having $\overline{\gamma}_r \to 0$.

Plugging both (27) and $\overline{\gamma}_r$ into (26) as a lower integration bound again yields

$$\mu_0 = 2\pi \cdot \rho \int_{s=0}^{\infty} \int_{\overline{\gamma}=\overline{\gamma}_r}^{\infty} P_S(\mathrm{tr}|\overline{\gamma}) \cdot f_{\overline{\gamma}}(\overline{\gamma}|s) \cdot s \cdot d\overline{\gamma} \cdot ds. \tag{28}$$

This is the basic formulation used in the next section to perform an analytic study of specific cases.

4. MEAN NODE DEGREE CLOSED-FORM DERIVATION

In this section, a closed-form derivation is proposed for the mean node degree in block-fading channels. The case of a simple AWGN channel is considered first. The results are then extended to block-fading channels.

4.1. Normalized node density

Albeit the exact expression provided above in (28) would permit to take shadowing into account, we decide to disregard it for enhancing the leading aim of this work, that is, the impact of unreliability on connectivity. Equation (28) therefore confines to

$$\mu_0 = 2\pi \cdot \rho \cdot \int_{s=0}^{d_r} P_S(\mathrm{tr}|\overline{\gamma}(d_{xx'} = s)) \cdot s \cdot ds, \tag{29}$$

where $d_r = d_0 \cdot (\overline{\gamma}_0/\overline{\gamma}_r)^{1/\alpha}$ corresponds to the distance at which $\overline{\gamma} = \overline{\gamma}_r$, and thus at which the successful transmission probability equals the reliability target P_{rel}.

In (29), the mean node degree depends on several system parameters: the node density ρ, the transmission power, and the noise level (all involved in $\overline{\gamma}(s)$). It is obvious that the connectivity of a network can be improved by either increasing the transmission power or the node density. Both have the same meaning from a graph point of view. A convenient generic formulation is proposed, relying on a different node density reference. Let d_1 be the distance at which the received power is unitary: $\overline{\gamma}(d_1) = 1$. $\overline{n}_1$ is then defined as the mean number of nodes located inside a disk of radius d_1:

$$\overline{n}_1 = \pi \cdot \rho \cdot d_1^2. \tag{30}$$

It is important to note that this distance depends physically on the path-loss parameters (α and L_0), the reception noise N_0, and the transmission power P_0, all defined in Section 2.2.

The mean SNR $\overline{\gamma}(d)$ is now expended from (10) as a function of d_1:

$$\overline{\gamma} = \left(\frac{d}{d_1}\right)^{-\alpha}. \tag{31}$$

A variable change from s to $\overline{\gamma}$ in (29) leads to

$$\mu_0 = \frac{2\overline{n}_1}{\alpha} \cdot \int_{\overline{\gamma}_r}^{\infty} \overline{\gamma}^{-(1+2/\alpha)} \cdot P_S(\mathrm{tr}|\overline{\gamma}) \cdot d\overline{\gamma}. \tag{32}$$

In (32), the mean node degree now only relies on one generic node density parameter $\overline{n}_1$, on the energy detection level through ε_d and on the attenuation parameter α.

4.2. Closed-form in AWGN

4.2.1. Transmission probability

Without fading, the mean SNR $\overline{\gamma}$ is merged in its instantaneous value γ. Then, $P_S(\mathrm{tr}|\gamma) = P_S(\mathrm{tr}|\overline{\gamma})$ and the integration lower bound in (32) is equal to $\max(\varepsilon_d, \overline{\gamma}_{\mathrm{th}})$. We assume that ε_d plays both roles in this case. Let us now focus on the instantaneous success probability $P_S(\mathrm{tr}|\gamma)$, which is directly related to the bit error rate (BER). A closed form of the BER is found in [32] for coherent detection in AWGN:

$$\mathrm{BER}(\gamma) = 0.5 \cdot \mathrm{erfc}\left(\sqrt{k \cdot \gamma}\right), \tag{33}$$

with $\mathrm{erfc}(x) = (2/\sqrt{\pi}) \cdot \int_{\sqrt{x}}^{\infty} e^{-u^2} du$, the complementary error function. k relies on the modulation kind and order, for example, $k = 1$ for binary phase shift keying (BPSK). The frame-based success probability is given in (23). Important for the following is the high SNR lower bound, valid for $(N_b \cdot \mathrm{BER}(\overline{\gamma})) \ll 0.1$:

$$P_S(\mathrm{tr}|\gamma) \sim 1 - N_b \cdot \mathrm{BER}(\gamma). \tag{34}$$

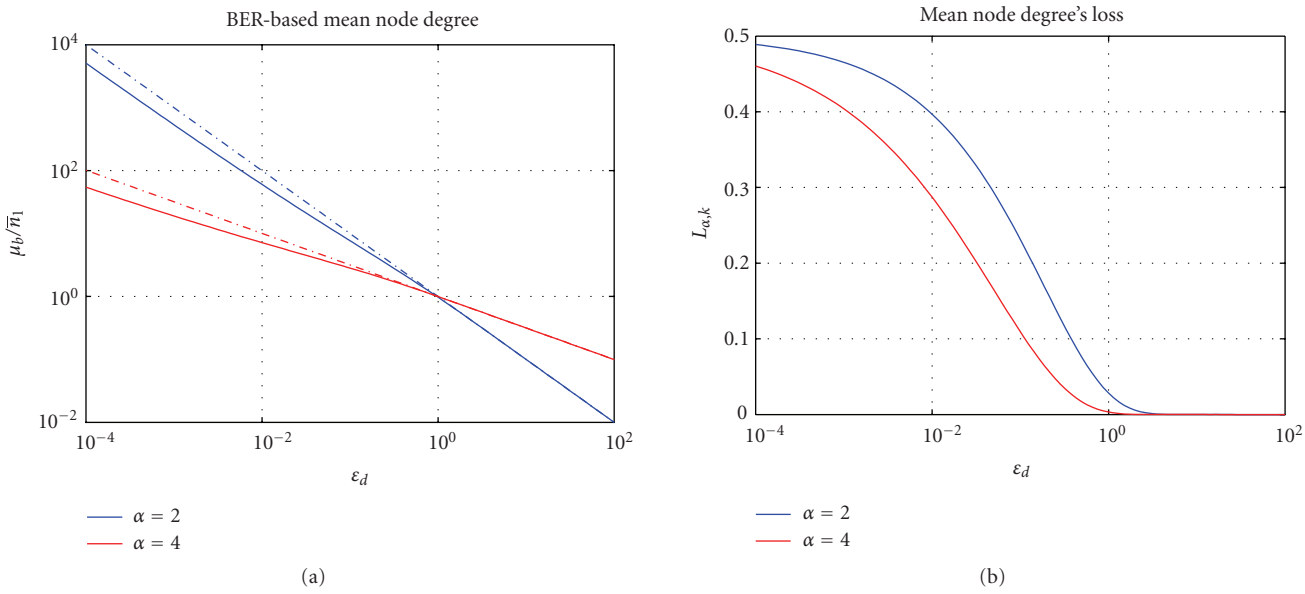

FIGURE 3: (a) The single-bit frame mean node degree is plotted as a function of ε_d for two attenuation slope coefficients ($\alpha = 2$ in blue, $\alpha = 4$ in red), having $k = 1$. The maximal mean node degree owing to a perfect switched link of the same range is also provided (dashed lines). (b) Connectivity loss $L_{\alpha,k}(\varepsilon_d)$ due to BER in the same conditions. The asymptotic mean node degree having $\varepsilon_d \to 0$ (i.e., when the range tends towards infinity) is half the switched link value, because the BER tends towards 0.5.

4.2.2. Single-bit frame derivation

Let us firstly evaluate the success probability for single-bit frames. This provides a mathematical basic result to be used later for larger frames.

The single bit based mean node degree μ_b is obtained as a function of ε_d by putting (23) having $N_b = 1$ into (32):

$$\mu_b(\varepsilon_d) = \frac{2\overline{n}_1}{\alpha} \cdot M_{\alpha,k}(\varepsilon_d), \tag{35}$$

with

$$M_{\alpha,k}(\varepsilon_d) = \int_{\gamma=\varepsilon_d}^{\infty} \gamma^{-(1+2/\alpha)} \cdot \left(1 - 0.5 \cdot \operatorname{erfc}\left(\sqrt{k \cdot \gamma}\right)\right) \cdot d\gamma. \tag{36}$$

After cumbersome computations detailed in the appendix, $M_{\alpha,k}(\varepsilon_d)$ is solved in (A.10), for $2 < \alpha < 4$. Basically, $M_{\alpha,k}(\varepsilon_d)$ could be easily solved for $\alpha \geq 4$, but this is kept out of the scope of this paper for the sake of conciseness.

The mean node degree which would be obtained under the switched link assumption and having the same range $d_{\varepsilon_d} = d_1 \cdot \varepsilon_d^{-1/\alpha}$ is given by plugging (30) into (13) as follows:

$$\mu_0(\varepsilon_d) = \overline{n}_1 \cdot \left(\frac{d_{\varepsilon_d}}{d_1}\right)^2, \tag{37}$$

which can be introduced in (A.10), making (35) equal to

$$\mu_b(\varepsilon_d) = \mu_0(\varepsilon_d) \cdot (1 - L_{\alpha,k}(\varepsilon_d)), \tag{38}$$

where $L_{\alpha,k}(\varepsilon_d)$ which denotes the mean node degree loss due to unreliability is

$$L_{\alpha,k}(\varepsilon_d) = 0.5 \cdot \operatorname{erfc}\left(\sqrt{k \cdot \varepsilon_d}\right) - \frac{\alpha}{(4-\alpha)\sqrt{\pi}} \cdot \left(\sqrt{k \cdot \varepsilon_d} \cdot e^{-k \cdot \varepsilon_d} - (k \cdot \varepsilon_d)^{2/\alpha} \left(\Gamma(\xi) - \Gamma_{\text{inc}}(\xi, k \cdot \varepsilon_d)\right)\right), \tag{39}$$

with $\xi = (3\alpha - 4)/2\alpha$. Γ and Γ_{inc} are, respectively, the well-known complete and incomplete gamma functions given by (A.8) and (A.9) in the appendix.

$\mu_b(\varepsilon_d)$ and $L_{\alpha,k}(\varepsilon_d)$ are plotted in Figure 3 for $k = 1$. $L_{\alpha,k}(\varepsilon_d)$ tends toward 0 (perfect transmission) and 0.5 (random reception) for short and long ranges, respectively. What is surprising at first glance is the divergence of $\mu_b(\varepsilon_d)$ when $\varepsilon_d \to 0$. This happens simply because the error transmission tends to 0.5 (and not 0). Thus, at long range, half of the nodes receive the right single bit. Let us now switch to the more meaningful case of N_b bits frames.

4.2.3. Frame-based first-order approximation

The frame-based mean node degree for N_b bits frames is denoted by μ_n. Plugging the exact success probability (23) into (32) provides

$$\mu_n(\varepsilon_d) = \frac{2\overline{n}_1}{\alpha} \cdot \int_{\varepsilon_d}^{\infty} \gamma^{-(1+2/\alpha)} \cdot (1 - \text{BER}(\gamma))^{N_b} \cdot d\gamma. \tag{40}$$

This result is illustrated for various parameters in Figure 4, thanks to numerical computations. As explained in

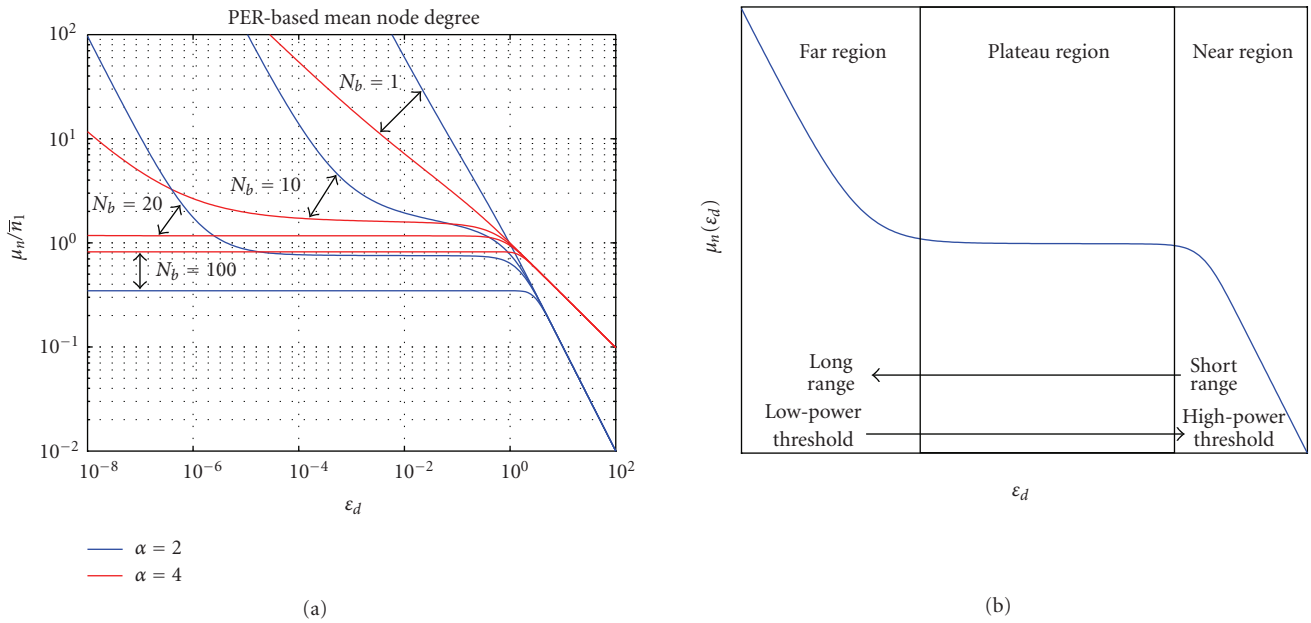

FIGURE 4: The curves represent the mean node degree as a function of the power detection level (ε_d) for $\alpha = 2$ (blue) and $\alpha = 4$ (red dashed). Each curve can be divided into three sections as illustrated in (b). Reading the chart from right to left, we have (i) the near section (high SNR threshold, low range), where the connectivity gets higher the less power threshold is used because the more range is achieved; (ii) the middle section where the curves reach a plateau. At this distance, the probability of having a new neighbor is negligible. Keeping N_b fixed, the plateau is reached whatever α is, approximately at the same SNR threshold, but stretches to a lower value for higher α; (iii) the far section (low SNR threshold, high range) for which the mean node degree diverges, having $\varepsilon_d \to 0$. At such a distance, the successful transmission probability decreases more slowly than the number of nodes grows. Basically, for a useful packet size ($Nb > 20$), the divergence region still mathematically exists but moves towards very low SNR values.

Figure 4(b), the mean node degree curves can be divided into the following three sections.

(i) Near section: for high SNR thresholds, the lower the power detection, the higher the mean node degree. The success probability is high and increasing the range (by decreasing the power detection level) provides an increased mean node degree.

(ii) Constant section: for intermediate threshold values, the mean node degree is constant. The reception probability for a node at this distance is very low. The nodes number in a ring at such a distance does not increase fast enough to compensate for the reliability leakage.

(iii) Far section: below a given threshold value, the reception probability tends to a constant value $\lim_{\gamma\to 0} P_s(\mathrm{tr}|\gamma) = 2^{-N_b}$, which corresponds to purely random reception. Since the number of neighbors tends to infinity, so is the number of successful transmissions.

The far zone is basically out of interest because transmissions are unforeseeable and a very low detection level would be required. These long hops are consequently poorly efficient from energy and resource sharing points of view. The near section is more interesting where the connectivity is improved by decreasing the detection level. The junction point between near and constant sections is proved to be a good tradeoff because it corresponds to the minimal neighborhood spreading achieving the plateau's value.

Let us further assume that the plateau is reached at a BER low enough to permit the use of (34) into (32). This provides an asymptotic lower bound for the mean node degree, denoted by $\widetilde{\mu}_n(\varepsilon_d)$ and given by

$$\widetilde{\mu}_n(\varepsilon_d) = \frac{2\overline{n}_1}{\alpha} \cdot \int_{\varepsilon_d}^{\infty} \gamma^{-(1+2/\alpha)} \cdot (1 - N_b \cdot \mathrm{BER}(\gamma)) \cdot d\gamma. \tag{41}$$

Using the definition (A.10) of $M_{\alpha,k}(\varepsilon_d)$ and the bit-based mean node degree (38) provides

$$\widetilde{\mu}_n(\varepsilon_d) = N_b \cdot \mu_b(\varepsilon_d) - (N_b - 1)\frac{2\overline{n}_1}{\alpha} \cdot \int_{\varepsilon_d}^{\infty} \gamma^{-(1+2/\alpha)} \cdot d\gamma, \tag{42}$$

which can be simplified as

$$\widetilde{\mu}_n(\varepsilon_d) = \mu_0(\varepsilon_d) \cdot (1 - N_b \cdot L_{\alpha,k}(\varepsilon_d)). \tag{43}$$

This approximation is assessed in Figure 5. The exact mean node degree is plotted (plain line) as a function of d_{ε_d}, the range at which $\gamma(d_{\varepsilon_d}) = \varepsilon_d$. The optimal mean node degree is equal to $0.197 \cdot \overline{n}_1$, reached when $d_{\varepsilon_d} \geq 0.5 \cdot d_1$. The proposed lower bound (43) (dashed line) is tight for $d_{\varepsilon_d} < 0.45 \cdot d_1$. The success probability provided in the upper frame shows that unreliable links (e.g., $P_s(\mathrm{tr}|\gamma) < 98\%$) represent about 30% of the whole connectivity. The needed tradeoff between reliability and connectivity is clearly illustrated.

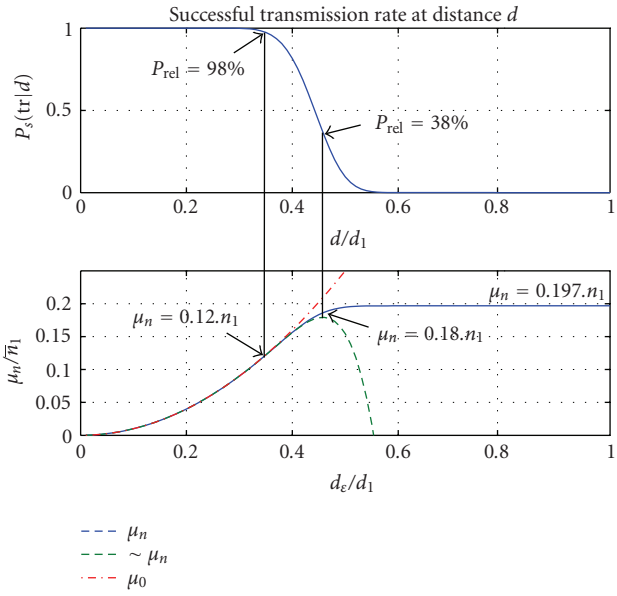

Figure 5: Upper frame: successful transmission probability as a function of the link distance. Lower frame: mean node degree as a function of the system range determined by the power detection level $d_\varepsilon = \varepsilon_d^{-1/\alpha} \cdot d_1$. The exact expression numerically estimated (blue, plain), the approximation according to (43) (green, dashed), and the ideal switched link expression (red, dash dotted) are provided. The optimal mean node degree (0.197) can be achieved at the price of having some unreliable radio links. The suboptimal analytic solution from (43) is close to the optimal connectivity, having a limit success probability equal to $P_{\text{rel}} = 38\%$. On the opposite, reliable links can be obtained at the price of a reduced connectivity. The mean node degree downshifts to 0.12. The simulation setup corresponds to a BPSK ($k = 1$), a free-space attenuation slope coefficient ($\alpha = 2$), and 1000-bit length frames.

4.2.4. Optimal power detection level

We now propose to find an analytic expression of the power detection threshold which performs a good tradeoff between reliability and connectivity.

The proposed lower bound (43) exhibits a maximal value located just beneath the plateau (see Figure 5). Because the plateau's value cannot be easily handled, this maximal value can be used to approximate the optimal SNR and the corresponding mean node degree by setting the first derivative of (43) to 0:

$$\frac{\partial \widetilde{\mu}_n(\varepsilon_d)}{\partial \varepsilon_d} = N_b \cdot \frac{\partial \mu_b(\varepsilon_d)}{\partial \varepsilon_d} + \frac{2}{\alpha}(N_b - 1) \cdot \overline{n}_1 \cdot \varepsilon_d^{-1-2/\alpha} = 0. \tag{44}$$

The derived of $\mu_b(\varepsilon_d)$ is obviously obtained from $M_{\alpha,k}(\varepsilon_d)$ and yields the following exact solution:

$$\widehat{\varepsilon}_d = \arg\max_{\varepsilon_d \in R^+}(\mu_n(\varepsilon_d)) = \frac{\left(\text{erfc}^{-1}(2/N_b)\right)^2}{k}, \tag{45}$$

where $\text{erfc}^{-1}(x)$ is the inverse of $\text{erfc}(x)$. For the example illustrated in Figure 5, one found $\mu_n(\widehat{\varepsilon}_d) = 0.18$.

An important result is that setting the power detection level to $\widehat{\varepsilon}_d$ optimizes the connectivity only when unreliable links are supported. The minimal success rate corresponding to longer hops downshifts to $P_s(\text{tr}|\widehat{\varepsilon}_d)$. It is further important to note that $\widehat{\varepsilon}_d$ does not rely on the path-loss coefficient α which means that the power detection level does not depend on the environment attenuation slope coefficient.

The optimal power detection level $\widehat{\varepsilon}_d$ from (45) is plotted in Figure 6 as a function of N_b. The corresponding mean node degree and range are also provided. In this figure $\widehat{d}_{\varepsilon_d}/d_1$ and $\mu_n(\varepsilon_d)/\overline{n}_1$ seem to be higher for a higher α. Basically, it is accounted for by the normalized density $\overline{n}_1$ used instead of ρ. $\overline{n}_1$ indeed relies on d_1, which in turn depends on path-loss properties.

In this section, we derived a close relationship between power detection level and radio link reliability. The connectivity increase due to the use of unreliable long hops is quantified. An analytic expression providing an optimal threshold value is proposed and proven independent of the environment attenuation slope coefficient. This provides the MAC layer with a manner to drive jointly link reliability and node degree depending on requests from the routing layer.

4.3. Nakagami-m block-fading channels

4.3.1. Radio link

This section now aims at extending the previous results to the case of block-fading channels described in Section 3.2. We propose the use of the Nakagami-m distributions [31, 32] which are often used for modeling fading in various conditions from AWGN ($m \to \infty$) to Rayleigh ($m = 1$). The SNR's pdf is given by

$$f_\gamma(\gamma|\overline{\gamma}) = \frac{m^m \cdot \gamma^{m-1}}{\Gamma(m) \cdot \overline{\gamma}^m} \exp\left(\frac{-m \cdot \gamma}{\overline{\gamma}}\right), \tag{46}$$

where $\Gamma(m)$ is the gamma function (see (A.8) in the appendix), and m drives the strength of the diffuse component.

4.3.2. Frame-based approximation

The success probability is given by (25). The mean node degree in block fading, namely μ_f, is derived from (32) as follows:

$$\mu_f(\overline{\gamma}_r, \varepsilon_d) = \frac{2\overline{n}_1}{\alpha} \cdot \int_{\overline{\gamma}_r}^{\infty} \overline{\gamma}^{-(1+2|\alpha)} \cdot \int_{\varepsilon_d}^{\infty} P_S(\text{tr}|\gamma) \cdot f_\gamma(\gamma|\overline{\gamma}) \cdot d\gamma \cdot d\overline{\gamma}. \tag{47}$$

Note that both thresholds ε_d and $\overline{\gamma}_r$ defined in Section 3.3 now differ from each other.

This double integral evaluated when $\overline{\gamma}_r \to 0$, as detailed in the appendix leads to

$$\mu_f(\overline{\gamma}_r \longrightarrow 0, \varepsilon_d) = \frac{2 \cdot \overline{n}_1}{\alpha} \cdot \frac{m^{-2|\alpha} \cdot \Gamma(m+2/\alpha)}{\Gamma(m)} \cdot \int_{\varepsilon_d}^{\infty} \gamma^{-(1+2/\alpha)} \cdot P_S(\text{tr}|\gamma) \cdot d\gamma. \tag{48}$$

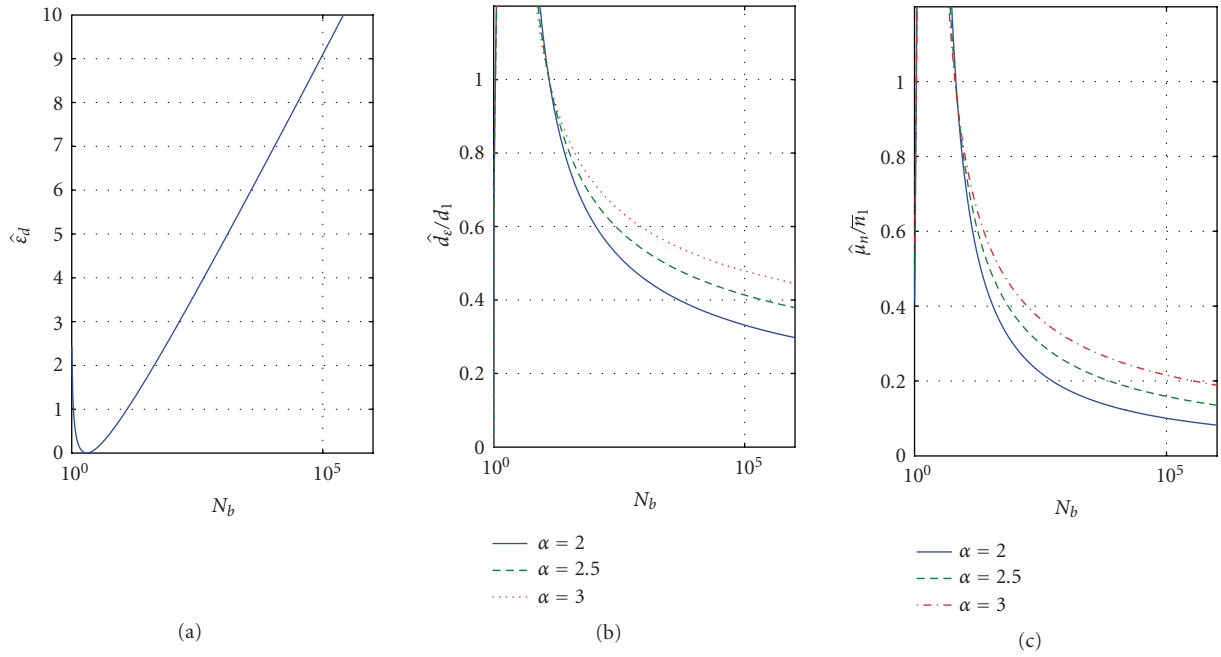

FIGURE 6: (a) Optimal power detection threshold as a function of frame size, (b) the corresponding range, and (c) mean node degree.

$\mu_f(\overline{\gamma}_r \to 0, \varepsilon_d)$ is referred to as the asymptotic mean node degree in the following and corresponds to the optimistic case when the WSN can exploit all neighbors whatever their reliability is.

The result provided in (48) has a significant meaning: the mean node degree experienced in a fading environment is very close to the one experienced in AWGN (with a same attenuation slope). Identifying (40) into (48) leads to

$$\mu_f(\overline{\gamma}_r \longrightarrow 0, \varepsilon_d) = C_{\text{loss}}(m, \alpha) \cdot \mu_n(\varepsilon_d), \tag{49}$$

where $\mu_n(\varepsilon_d)$ is the mean node degree in AWGN channel and $C_{\text{loss}}(m, \alpha)$ is a connectivity loss coefficient illustrated in Figure 7 and extracted from (47) as

$$C_{\text{loss}}(m, \alpha) = \frac{m^{-2/\alpha} \cdot \Gamma(m + 2/\alpha)}{\Gamma(m)}. \tag{50}$$

It is interesting to note that this coefficient relies neither on k, nor on N_b.

The asymptotic mean node degree is now approximated by putting (43) into (49), leading to

$$\widetilde{\mu}_f(\overline{\gamma}_r \longrightarrow 0, \varepsilon_d) = C_{\text{loss}}(m, \alpha) \cdot \widetilde{\mu}_n(\varepsilon_d). \tag{51}$$

A first noticeable result found for $\alpha = 2$ (perfect free-space model) is that the mean node degree proves independent on fading strength ($C_{\text{loss}}(m, 2) = 1$; for all m). It reveals that new random far links exactly compensate for link loss in the near range. For higher values of α, a weak negative imbalance of about 10% is achieved in a Rayleigh channel ($m = 1$), which is the more severe channel arising in indoor-like environments.

A second important result is that the proposed power detection level $\widehat{\varepsilon}_d$ obtained in (45) for AWGN is further efficient

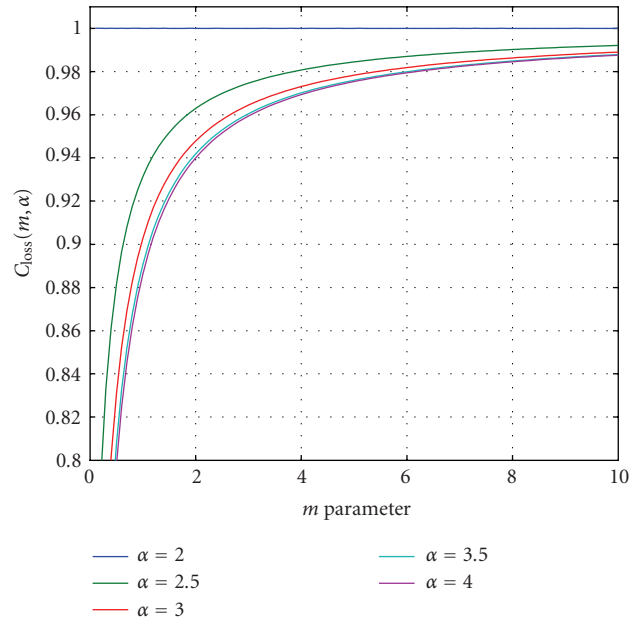

FIGURE 7: $C_{\text{loss}}(m, \alpha)$ is represented as a function of the parameter m of the Nakagami-m distribution and for various attenuation slope coefficients α. It represents the connectivity loss due to block fading.

for any fading environment (for all m) and any propagation model (for all α; $2 \le \alpha < 4$). Therefore $\widehat{\varepsilon}_d$ makes the mean node degree close to optimal according to

$$\widehat{\mu}_f(\overline{\gamma}_r \longrightarrow 0, \varepsilon_d) = C_{\text{loss}}(m, \alpha) \cdot \mu_0(\widehat{\varepsilon}_d) \cdot (1 - N_b \cdot L_{\alpha,k}(\widehat{\varepsilon}_d)). \tag{52}$$

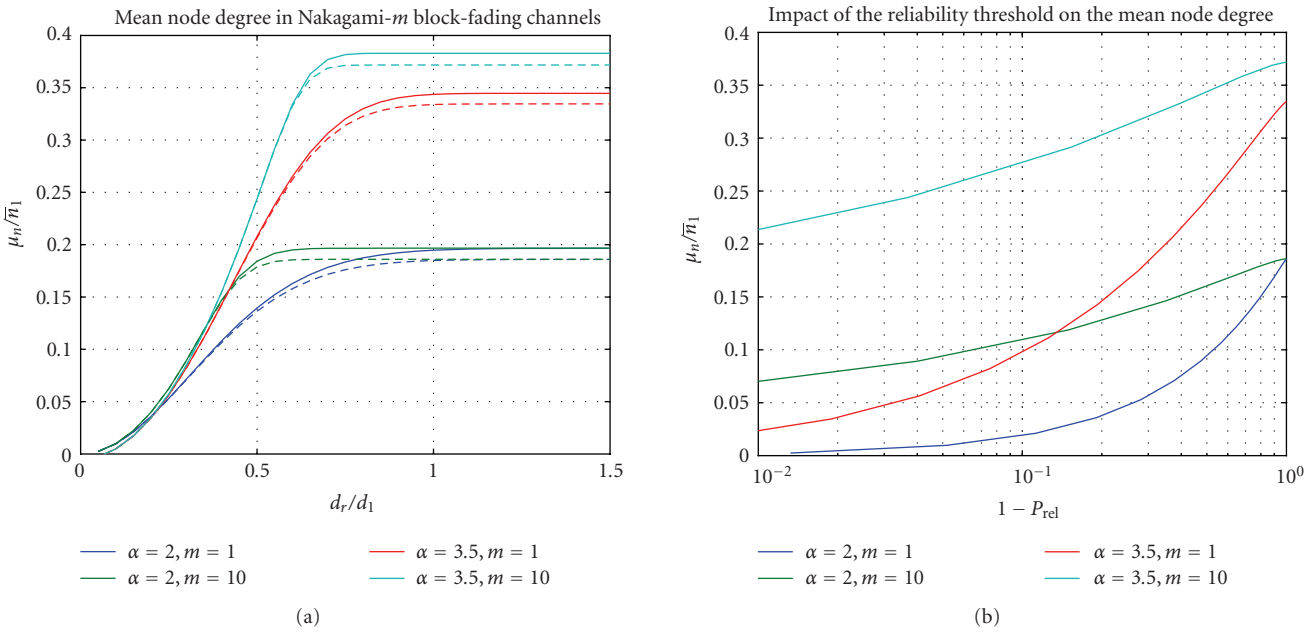

FIGURE 8: Mean node degree estimation for a BPSK modulation ($k = 1$), with $N_b = 1000$ bits, plotted as a function of the reliability range, d_r in (a), and the limit transmission error probability $P_{\text{err}}(\text{tr}|\overline{\gamma}_r) = 1 - P_{\text{rel}}$ in (b). In (a), the curves are numerically obtained from (47), with a different power detection threshold $\varepsilon_d ll \hat{\varepsilon}_d$ (plain) and $\varepsilon_d = \hat{\varepsilon}_d$ (dotted curves). In (b), the connectivity loss owing to a reliability threshold is plotted. For instance, a reliability need of $P_{\text{err}}(\text{tr}) < 10\%$ would make the mean node degree decreasing from 0.2 to 0.015 with $m = 1$ and $\alpha = 2$.

However, both results do not mean that fading has no effect on connectivity. The mean node degree is plotted in Figure 8(a) as a function of d_r, the distance at which the mean power is equal to the reliability threshold $\overline{\gamma}_r$. Plain and dashed plots hold for the exact mean node degree from (47) computed numerically having, respectively, $\varepsilon_d = \epsilon; \epsilon \ll \hat{\varepsilon}_d$ and $\varepsilon_d = \hat{\varepsilon}_d$ from (45). The weak connectivity loss is due to the power detection threshold. These curves are provided for 4 pairs (α, m). For $\alpha = 2$, the same asymptotic value is reached for any m value, but further away in Rayleigh conditions. It means that the neighborhood stretches with increasing fading, making the links less reliable.

Figure 8(b) shows the same curves as a function of the reliable probability limit P_{rel}. The connectivity leakage owing to a stringent P_{rel} is seen, especially for strong fading. With $\alpha = 2$, the maximal connectivity is equal to 0.19, whatever m. A constraint of $P_{\text{rel}} = 0.9$ is fulfilled having a mean node degree going down to 0.11 and 0.02 for $m = 10$ and $m = 1$, respectively. The capability of managing unreliable links is thus a very important feature for WSNs roll out in strong fading environments.

In this section, the asymptotic mean node degree was firstly expressed as a function of the mean node degree in AWGN weighted by a loss factor. The weakness of the loss factor was observed. A lower bound of the asymptotic mean node degree was also provided. Secondly, the optimal power detection threshold ε_d analytically derived in previous section for AWGN was found still valid whatever the fading strength is. Lastly, the effect of fading on reliability has been assessed.

The leading conclusion is that unreliable links may contribute significantly to improve the connectivity of a WSN.

5. SIMULATION RESULTS

The theoretical analysis of the previous section is now validated by extensive simulation. Section 5.1 describes the simulation setup. In Section 5.2, the mean node degree study is compared to simulations. Then, in Section 5.3 the tightness of the connectivity bound provided by (5) in Section 2 is evaluated.

5.1. Simulation setup

Mean node degree and connectivity were evaluated in a disk area A with surface S_A. The complete roll-out simulation area Ω is a larger disk including A. The node degree of all nodes in A is evaluated, taking into account all the nodes in Ω in order to avoid boundary problems and to simulate A as a subpart of an infinite network [21]. From a practical point of view, we found it reliable enough to choose Ω as a disk having radius $(R_\Omega = 2 \cdot R_A)$.

In the simulations, the average number of nodes in A is kept constant. We have the normalized node density $\overline{n}_1$ vary by varying the transmission power. Note that the radius of the unitary received power area (d_1) changes accordingly. This choice is equivalent to modifying the node density, but with our approach, we keep the mean number of simulated nodes constant.

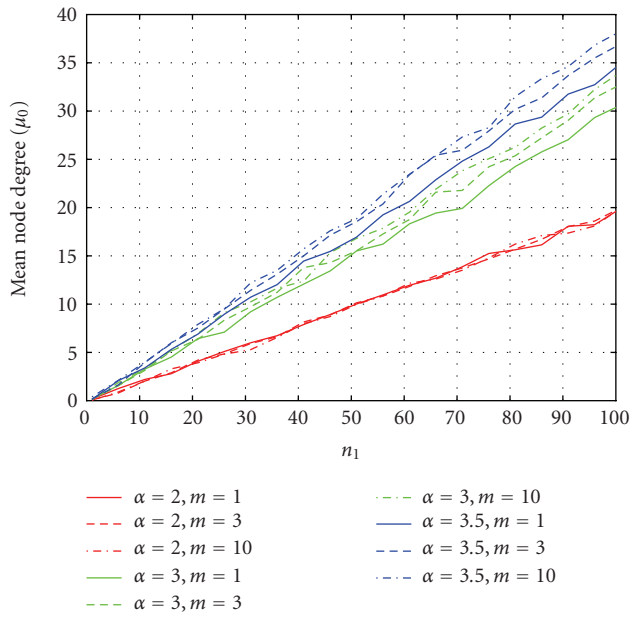

FIGURE 9: Simulated mean node degree in Nakagami-m channels as a function of the relative node density.

When not specified, the simulations results presented below were obtained with default parameters set to $k = 1$ (BPSK modulation), a path-loss coefficient $\alpha = 2$ (free-space conditions), and a frame size of 1000 bits. The mean number of nodes in A equals 50. For each transmission power level, 100 random sets of nodes were generated. For each set, the pairwise connection matrix was computed 20 times, independently. The number of nodes is Poisson distributed, and they are randomly and uniformly distributed over the whole space.

5.2. Mean node degree

The mean node degree is firstly investigated. Figure 9 shows the relative mean node degree $\overline{\mu}_n/\overline{n}_1$ as given by (49). Average simulation results are provided for Nakagami-m channels using different coefficient attenuation α. The relationship is found linear as expected from the previous section. For $\alpha = 2$ the mean node degree is not dependent on m which fits the theoretical results. This group of curves further emphasizes the weak dependency to fading of the mean node degree. As stated above, this result will be experienced by a WSN, only if it is able to deal with opportunistic transmissions. For $\alpha = 3$ and $\alpha = 3.5$ the mean node degree's loss corresponds to the C_{loss} coefficient computed above. In order to verify the theoretical result of (47), the simulations corresponding are carried out. Figures 10(a) and 10(b) are the simulation results for $\alpha = 2$ and $\alpha = 3.5$, respectively, in various channel conditions AWGN, Rayleigh and Nakagami-m. These results concord with theoretical results shown in previous section. These curves confirm that in Rayleigh channels, comparing with AWGN, the long hops have an important role to compensate the loss of short hops. To check the impact of the power detection level $\widehat{\varepsilon}_d$ on the mean node degree, the simulations are performed for three power detection threshold values: $\varepsilon_d = 0$, $\varepsilon_d = \widehat{\varepsilon}_d$, and $\varepsilon_d = 2\widehat{\varepsilon}_d$. Figure 11 displays that the mean node degree reduces of 5%; however, when $\varepsilon_d = 2\widehat{\varepsilon}_d$, the mean node degree goes down of 48%. $\widehat{\varepsilon}_d$, according to (45) proves to be close to the optimal power detection threshold. These results simultaneously show how increasing the detection threshold deletes long hops.

5.3. Connectivity probability

Albeit the mean node degree is constant, the graph associated with a WSN is very sensitive to the fading strength. First of all, Figure 8(a) has shown that the connected neighborhood of a node spreads out with fading: the mean length of hops increases. Figure 12 illustrates the random graphs for AWGN and Rayleigh conditions. In the second case, some long hops are seen and the structure appears less homogeneous.

Note that in this figure, the inner circle represents the area of interest A and contains all the nodes for which the connectivity is evaluated. The outer nodes contained in the second circle are used only as relay for connecting inner nodes. This illustrates how the boundary problem is overcome in this approach.

Figure 13 represents the mean connectivity experienced in our simulations. As found in previous section, the nonisolated node probability relying on the mean node degree is not affected by fading whatever m. Basically, the nonisolated node probability acts as an upper bound for the connectivity: a network cannot be connected if just one node is isolated. This figure also shows that the bound gets tighter the more the fading strength is.

Fading indeed changes the graph from a pure geometric graph to a random graph. The mean number of links is constant whatever m is, but fading favors longer links which are more efficient to maintaining the network connectivity. The conclusions are twofold:

(i) the mean path-loss function is sufficient to predicting the mean node degree and thus the nonisolated node probability,

(ii) second-order variations of the received power due to fading do not change the mean node degree and allow to improve the connectivity.

6. CONCLUSIONS

This work is based on the framework proposed by Bettstetter et al., as described in Section 2. The main novelty rests on the relaxation of the switched-link model. For this purpose, an instantaneous node degree was defined. Its expectation leads to a mean node degree definition representing the mean number of simultaneous successful receptions of a packet. The main difference with the classical definition is taking into account random transmission losses. Furthermore, several parameters were introduced in the model such as fading strength, modulation kind or frame size. Moreover, two threshold parameters managed by the MAC or the

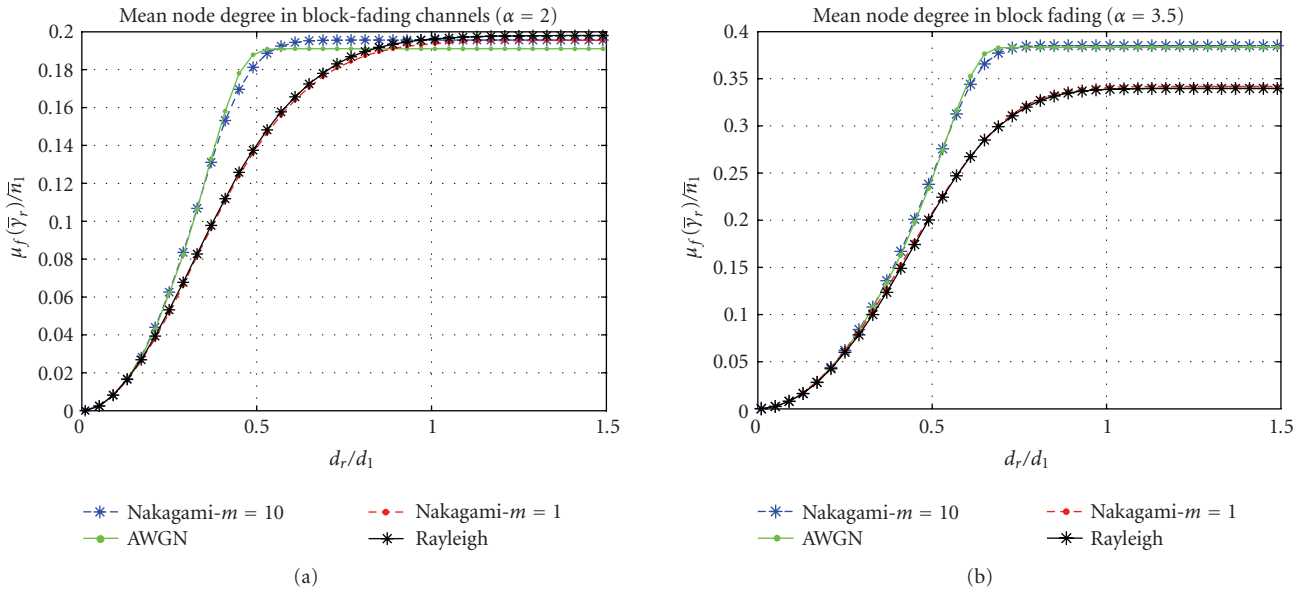

Figure 10: Related mean node degree in Nakagami-m, AWGN, Rayleigh channels as function of the reliability range d_r, with $\alpha = 2$ (a) and $\alpha = 3.5$ (b).

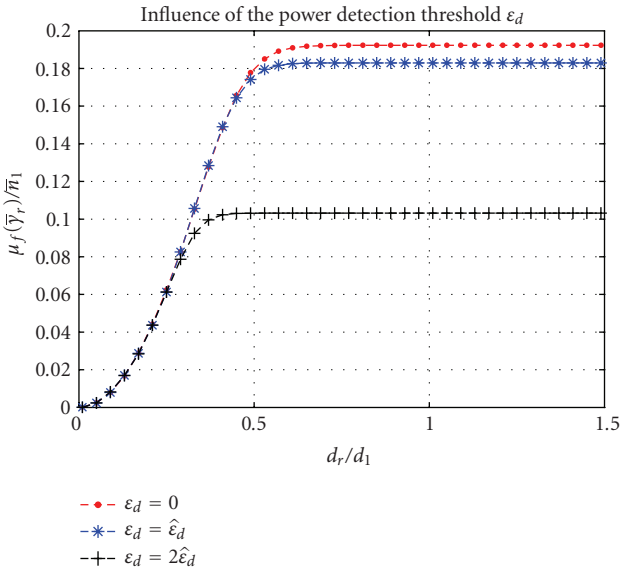

Figure 11: Related mean node degree in Nakagami-m, $m = 10$, channels for different ε_d as function of the reliability range d_r ($\alpha = 2$).

routing layers were also introduced. The first was the power detection level, the second was the link reliability threshold.

In Section 3, we first defined a normalized node density $\overline{n}_1$ as the number of nodes included in a disk of radius d_1 such as $\gamma(d_1) = 1$. This convenient definition provided the mean node degree proportional to one scaling parameter only, $\overline{n}_1$, bringing together the noise level, the mean path-loss, the transmission power, and the node density. Then, the AWGN case was deeply studied in Section 4.2. A lower bound of the mean node degree was found as a function of the power detection level. An analytic expression was further proposed for a weakly suboptimal power detection level. The corresponding link reliability was also evaluated and analyzed. These results were finally broadened for block-fading channels in Section 4.3 and the tradeoff between connectivity and link reliability was widely studied. The theoretical results were validated by simulation in Section 5.

An important result was found stating that the suboptimal power detection level was valid whatever were the fading strength and the path-loss attenuation slope coefficient. Thus, the proposed power detection level does not rely on environment properties. We also observed that fading weakly reduces the mean node degree but spreads the neighbors over a wider area, making the links less reliable.

Simulations have exhibited fading has a positive effect on connectivity. Indeed, for a same mean node degree value, connectivity in fading channels is closer to the no-node-isolation probability.

This work clearly advocates for long hops routing as discussed in [34] and more likely for opportunistic routing. From all these results, developing protocols able to exploit unreliable links appear indeed challenging. This is an important issue for WSN, because improving the connectivity allows the number of active nodes to be smaller, thus increasing the life time. Basically, increasing the connectivity by using an opportunistic transmission over several paths is nothing else than a distributed extension of the well-known diversity principle usually used in mobile communications to enhance individual radio links.

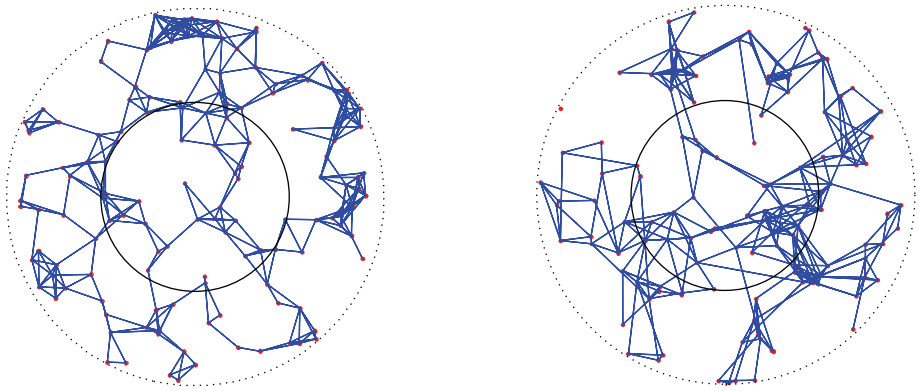

(a) AWGN channel (b) Rayleigh channel

Figure 12: A peculiar realization of graphs is given for (a) AWGN and (b) Rayleigh conditions, with about 50 nodes in the smaller disk. Albeit the mean node degree is constant (equal to 7.5), higher length hops in Rayleigh channels make the network better connected.

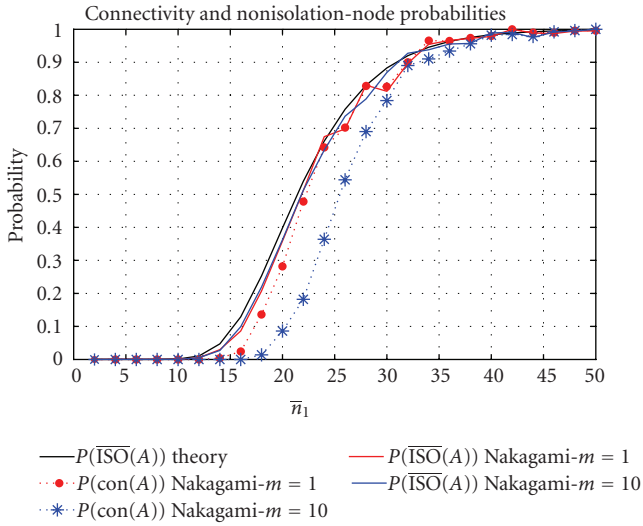

Figure 13: Connectivity under block fading, AWGN ($m > 10$) and Rayleigh ($m = 1$) conditions. The connectivity and the nonisolated node probabilities have been assessed by simulation. The theoretical nonisolated node probability according to (3) for the approximated mean node degree given in (49) is also provided.

APPENDIX

A. BER-BASED DERIVATION OF THE MEAN NODE DEGREE

A.1. Derivation in AWGN channel

Computing the BER-based mean node degree in AWGN from (35) holds on computing $M_{\alpha,k}(\varepsilon_d)$ defined in (36) which can be divided in two parts:

$$M_{\alpha,k}(\varepsilon_d) = \int_{\varepsilon_d}^{\infty} \gamma^{-(1+2/\alpha)} \cdot d\gamma - \frac{1}{\sqrt{\pi}} A_{\alpha,k}(\varepsilon_d), \tag{A.1}$$

where

$$A_{\alpha,k}(\varepsilon_d) = \int_{\gamma=\varepsilon_d}^{\infty} \gamma^{-(1+2/\alpha)} \cdot \int_{x=\sqrt{k\cdot\gamma}}^{\infty} e^{-x^2} \cdot dx \cdot d\gamma. \tag{A.2}$$

Applying Fubini's theorem to $A_{\alpha,k}(\varepsilon_d)$ yields

$$A_{\alpha,k}(\varepsilon_d) = \int_{x=\sqrt{k\cdot\varepsilon_d}}^{\infty} e^{-x^2} \int_{\gamma=\varepsilon_d}^{x^2/k} \gamma^{-(1+2/\alpha)} \cdot d\gamma \cdot dx. \tag{A.3}$$

The integration with respect to γ is easily computed providing

$$A_{\alpha,k}(\varepsilon_d) = \frac{\alpha\sqrt{\pi}}{4} \cdot \varepsilon_d^{-2/\alpha} \cdot \operatorname{erfc}\left(\sqrt{k\cdot\varepsilon_d}\right) - \frac{\alpha}{2} \cdot k^{2/\alpha} \cdot B_{\alpha,k}(\varepsilon_d), \tag{A.4}$$

where

$$B_{\alpha,k}(\varepsilon_d) = \int_{\sqrt{k\cdot\varepsilon_d}}^{\infty} x^{-4/\alpha} \cdot e^{-x^2} \cdot dx. \tag{A.5}$$

$B_{\alpha,k}(\varepsilon_d)$ looks like a gamma function but with a negative power exponent $(-4/\alpha)$ making the integral divergent for $\alpha < 4$ while the most usual values of α are comprised between 2 and 4. To achieve a closed form, this integral can be integrated by parts leading to

$$B_{\alpha,k}(\varepsilon_d) = \frac{\alpha}{4-\alpha}\left((k\cdot\varepsilon_d)^{(\alpha-4)/2\alpha} \cdot e^{-k\cdot\varepsilon_d} - \int_{k\cdot\varepsilon_d}^{\infty} u^{1/2-2/\alpha} \cdot e^{-u} \cdot du\right). \tag{A.6}$$

The second integral is now a convergent gamma function (for $\alpha \geq 2$), providing

$$B_{\alpha,k}(\varepsilon_d) = \frac{\alpha}{4-\alpha}\left((k\cdot\varepsilon_d)^{(\alpha-4)/2\alpha} \cdot e^{-k\cdot\varepsilon_d} - \Gamma\left(\frac{3}{2} - \frac{2}{\alpha}\right) + \Gamma_{\text{inc}}\left(\frac{3}{2} - \frac{2}{\alpha}, k\cdot\varepsilon_d\right)\right), \tag{A.7}$$

having $\Gamma(\xi)$ the usual gamma function defined as

$$\Gamma(\xi) = \int_0^\infty t^{\xi-1} \cdot e^{-t} \cdot dt \tag{A.8}$$

and $\Gamma_{\text{inc}}(\xi, x)$ the usual incomplete gamma function defined as

$$\Gamma_{\text{inc}}(\xi, x) = \int_0^x t^{\xi-1} \cdot e^{-t} \cdot dt. \tag{A.9}$$

Reporting $B_{\alpha,k}(\varepsilon_d)$ into $A_{\alpha,k}(\varepsilon_d)$ and then into $M_{\alpha,k}(\varepsilon_d)$ provides the exact expression

$$M_{\alpha,k}(\varepsilon_d) = \frac{\alpha}{2}\Bigg[\varepsilon_d^{-2/\alpha} \cdot \left(1 - 0.5 \cdot \text{erfc}\left(\sqrt{k \cdot \varepsilon_d}\right)\right) + \frac{\alpha}{(4-\alpha)\sqrt{\pi}}\left(\sqrt{k}\varepsilon_d^{(\alpha-4)/2\alpha} e^{-k\cdot\varepsilon_d} - k^{2/\alpha}(\Gamma(\xi) - \Gamma_{\text{inc}}(\xi, k \cdot \varepsilon_d))\right)\Bigg], \tag{A.10}$$

with $\xi = (3\alpha - 4)/2\alpha$.

A.2. Derivation in Nakagami-m channel

The mean node degree in Nakagami-m block-fading channels given by (47) can be written as

$$\mu_f(\overline{\gamma}_r, \varepsilon_d) = \frac{2\overline{n}_1}{\alpha} \cdot M'_{\alpha,k}(\overline{\gamma}_r, \varepsilon_d), \tag{A.11}$$

having (thanks to the Fubini's theorem)

$$M'_{\alpha,k}(\overline{\gamma}_r, \varepsilon_d) = \int_{\varepsilon_d}^\infty P_S(\text{tr}|\gamma) \cdot C_{\alpha,k}(\overline{\gamma}_r, \gamma) d\gamma, \tag{A.12}$$

where

$$C_{\alpha,k}(\overline{\gamma}_r, \gamma) = \int_{\overline{\gamma}_r}^\infty \overline{\gamma}^{-(1+2/\alpha)} \cdot f_\gamma(\gamma|\overline{\gamma}) \cdot d\overline{\gamma}. \tag{A.13}$$

Introducing the Nakagami-m pdf leads to

$$C_{\alpha,k}(\overline{\gamma}_r, \gamma) = \frac{m^m \cdot \gamma^{m-1}}{\Gamma(m)} \int_{\overline{\gamma}_r}^\infty \overline{\gamma}^{-(1+m+2/\alpha)} \cdot e^{(-m\cdot\gamma/\overline{\gamma})} \cdot d\overline{\gamma}. \tag{A.14}$$

An appropriate variable change leads to:

$$C_{\alpha,k}(\overline{\gamma}_r, \gamma) = \frac{m^{-2/\alpha} \cdot \gamma^{-(1+2/\alpha)}}{\Gamma(m)} \int_0^{m\gamma/\overline{\gamma}_r} t^{(m-1+2/\alpha)} \cdot e^{-t} \cdot dt. \tag{A.15}$$

The remaining integral is nothing else than the incomplete gamma function $\Gamma_{\text{inc}}(m + 2/\alpha, m\gamma/\overline{\gamma}_r)$ as defined in (A.9). Plugging (A.15) into (A.12) provides

$$M'_{\alpha,k}(\overline{\gamma}_r, \varepsilon_d) = \frac{m^{-2/\alpha} \cdot \Gamma(m + 2/\alpha)}{\Gamma(m)} \cdot \int_{\varepsilon_d}^\infty \gamma^{-(1+2/\alpha)} \cdot P_S(\text{tr}|\gamma) \cdot \frac{\Gamma_{\text{inc}}(m + 2/\alpha, m\gamma/\overline{\gamma}_r)}{\Gamma(m + 2/\alpha)} \cdot d\gamma. \tag{A.16}$$

Finally, when $\overline{\gamma}_r$ tends toward 0, one has

$$M'_{\alpha,k}(\overline{\gamma}_r \longrightarrow 0, \varepsilon_d) = \frac{m^{-2/\alpha} \cdot \Gamma(m + 2/\alpha)}{\Gamma(m)} \cdot \int_{\varepsilon_d}^\infty \gamma^{-(1+2/\alpha)} \cdot P_S(\text{tr}|\gamma) \cdot d\gamma. \tag{A.17}$$

ACKNOWLEDGMENTS

This work was done in the framework of the ARC IRAMUS Project of INRIA. This work was also partially supported by the French Ministry of Research under Contract ARESA ANR-05-RNRT-01703.

REFERENCES

[1] D. Simplot-Ryl, I. Stojmenovic, and J. Wu, "Energy-efficient backbone construction, broadcasting, and area coverage in sensor networks," in *Handbook of Sensor Networks*, I. Stojmenovic, Ed., pp. 343–380, John Wiley & Sons, New York, NY, USA, 2005.

[2] D. Tian and N. D. Georganas, "A coverage-preserving node scheduling scheme for large wireless sensor networks," in *Proceedings of the 1st ACM International Workshop on Wireless Sensor Networks and Applications (WSNA '02)*, pp. 32–41, Atlanta, Ga, USA, September 2002.

[3] A. Gallais, J. Carle, D. Simplot-Ryl, and I. Stojmenovic, "Localized sensor area coverage with low communication overhead," in *Proceedings of the 4th Annual IEEE International Conference on Pervasive Computing and Communications (PerCom '06)*, pp. 328–337, Pisa, Italy, March 2006.

[4] J. Carle, A. Gallais, and D. Simplot-Ryl, "Preserving area coverage in wireless sensor networks by using surface coverage relay dominating sets," in *Proceedings of the 10th IEEE Symposium on Computers and Communications (ISCC '05)*, pp. 347–352, Murcia, Cartagena, Spain, June 2005.

[5] E. M. Royer and C.-K. Toh, "A review of current routing protocols for ad hoc mobile wireless networks," *IEEE Personal Communications*, vol. 6, no. 2, pp. 46–55, 1999.

[6] O. Dousse and P. Thiran, "Connectivity vs capacity in dense ad hoc networks," in *Proceedings of the 23rd Annual Joint Conference of IEEE Computer and Communications Societies (INFOCOM '04)*, vol. 1, pp. 476–486, Hongkong, March 2004.

[7] O. Dousse, P. Thiran, and M. Hasler, "Connectivity in ad-hoc and hybrid networks," in *Proceedings of the 21st Annual Joint Conference of IEEE Computer and Communications Societies (INFOCOM '02)*, vol. 2, pp. 1079–1088, New York, NY, USA, June 2002.

[8] P. Gupta and P. R. Kumar, "The capacity of wireless networks," *IEEE Transactions on Information Theory*, vol. 46, no. 2, pp. 388–404, 2000.

[9] P. Gupta and P. R. Kumar, "Crtical power for asymptotic connectivity in wireless networks," in *Stochastic Analysis Control Optimization and Applications*, W. M. McEneany, G. Yin, and Q. Zhang, Eds., pp. 547–566, Birkhauser, Boston, Mass, USA, 1998.

[10] Y.-C. Cheng and T. G. Robertazzi, "Critical connectivity phenomena in multihop radio models," *IEEE Transactions on Communications*, vol. 37, no. 7, pp. 770–777, 1989.

[11] P. Piret, "On the connectivity of radio networks," *IEEE Transactions on Information Theory*, vol. 37, no. 5, pp. 1490–1492, 1991.

[12] P. Santi, "The critical transmitting range for connectivity in mobile ad hoc networks," *IEEE Transactions on Mobile Computing*, vol. 4, no. 3, pp. 310–317, 2005.

[13] M. Desai and D. Manjunath, "On the connectivity in finite ad hoc networks," *IEEE Communications Letters*, vol. 6, no. 10, pp. 437–439, 2002.

[14] C. Bettstetter, "On the minimum node degree and connectivity of a wireless multihop network," in *Proceedings of the 3rd ACM International Symposium on Mobile Ad Hoc Networking and Computing (MobiHoc '02)*, pp. 80–91, Lausanne, Switzerland, June 2002.

[15] C. Bettstetter, "On the connectivity of ad hoc networks," *The Computer Journal*, vol. 47, no. 4, pp. 432–447, 2004.

[16] A. P. Jardosh, E. M. Belding-Royer, K. C. Almeroth, and S. Suri, "Real-world environment models for mobile network evaluation," *IEEE Journal on Selected Areas in Communications*, vol. 23, no. 3, pp. 622–632, 2005.

[17] N. Sadagopan, F. Bai, B. Krishnamachari, and A. Helmy, "PATHS: analysis of PATH duration statistics and their impact on reactive MANET routing protocols," in *Proceedings of the 4th ACM International Symposium on Mobile Ad Hoc Networking and Computing (MobiHoc '03)*, pp. 245–256, Annapolis, Md, USA, June 2003.

[18] M. Takai, R. Bagrodia, K. Tang, and M. Gerla, "Efficient wireless network simulations with detailed propagation models," *Wireless Networks*, vol. 7, no. 3, pp. 297–305, 2001.

[19] G. Zhou, T. He, S. Krishnamurthy, and J. A. Stankovic, "Models and solutions for radio irregularity in wireless sensor networks," *ACM Transactions on Sensor Networks*, vol. 2, no. 2, pp. 221–262, 2006.

[20] I. Stojmenovic, A. Nayak, and J. Kuruvila, "Design guidelines for routing protocols in ad hoc and sensor networks with a realistic physical layer," *IEEE Communications Magazine*, vol. 43, no. 3, pp. 101–106, 2005.

[21] C. Bettstetter and C. Hartmann, "Connectivity of wireless multihop networks in a shadow fading environment," *Wireless Networks*, vol. 11, no. 5, pp. 571–579, 2005.

[22] R. Hekmat and P. van Mieghem, "Study of connectivity in wireless ad-hoc networks with an improved radio model," in *Proceedings of the 2nd Workshop on Modeling and Optimization in Mobile, Ad Hoc and Wireless Networks (WiOpt '04)*, pp. 1–10, Cambridge, UK, March 2004.

[23] D. Miorandi and E. Altman, "Coverage and connectivity of ad hoc networks presence of channel randomness," in *Proceedings of the 24th Annual Joint Conference of the IEEE Computer and Communications Societies (INFOCOM '05)*, vol. 1, pp. 491–502, Miami, Fla, USA, March 2005.

[24] J. Zhang and S. C. Liew, "Capacity improvement of wireless ad hoc networks with directional antennae," in *Proceedings of the 63rd IEEE Vehicular Technology Conference (VTC '06)*, vol. 2, pp. 911–915, Melbourne, Australia, May-July 2006.

[25] C. Bettstetter, C. Hartmann, and C. Moser, "How does randomized beamforming improve the connectivity of ad hoc networks?" in *IEEE International Conference on Communications (ICC '05)*, vol. 5, pp. 3380–3385, Seoul, South Korea, May 2005.

[26] O. Dousse, F. Baccelli, and P. Thiran, "Impact of interferences on connectivity in ad hoc networks," *IEEE/ACM Transactions on Networking*, vol. 13, no. 2, pp. 425–436, 2005.

[27] H. Karvonen, Z. Shelby, and C. Pomalaza-Raez, "Coding for energy efficient wireless embedded networks," in *Proceedings of the International Workshop on Wireless Ad-Hoc Networks (IWWAN '04)*, pp. 300–304, Oulu, Finland, May-June 2004.

[28] Y. Sankarasubramaniam, I. F. Akyildiz, and S. W. McLaughlin, "Energy efficiency based packet size optimization in wireless sensor networks," in *Proceedings of the 1st IEEE International Workshop on Sensor Network Protocols and Applications (SNPA '03)*, pp. 1–8, Anchorage, Alaska, USA, May 2003.

[29] M. Franceschetti, L. Booth, M. Cook, R. Meester, and J. Bruck, "Continuum percolation with unreliable and spread-out connections," *Journal of Statistical Physics*, vol. 118, no. 3-4, pp. 721–734, 2005.

[30] A. Neskovic, N. Neskovic, and G. Paunovic, "Modern approaches in modeling of mobile radio systems propagation environment," *IEEE Communications Surveys & Tutorials*, vol. 3, no. 3, pp. 2–12, 2000.

[31] S. R. Saunders, *Antennas and Propagation for Wireless Communication Systems*, John Wiley & Sons, New York, NY, USA, 1999.

[32] Z. Wang and G. B. Giannakis, "A simple and general parametrization quantifying performance in fading channels," *IEEE Transactions on Communications*, vol. 51, no. 8, pp. 1389–1398, 2003.

[33] F. Ye, G. Zhong, S. Lu, and L. Zhang, "GRAdient broadcast: a robust data delivery protocol for large scale sensor networks," *Wireless Networks*, vol. 11, no. 3, pp. 285–298, 2005.

[34] M. Haenggi and D. Puccinelli, "Routing in ad hoc networks: a case for long hops," *IEEE Communications Magazine*, vol. 43, no. 10, pp. 93–101, 2005.